

Conductive collagen/polypyrrole-b-polycaprolactone hydrogel for bioprinting of neural tissue constructs

Sanjairaj Vijayavenkataraman*, Novelia Vialli, Jerry Y. H. Fuh, Wen Feng Lu*

Department of Mechanical Engineering, National University of Singapore, Singapore

Abstract: Bioprinting is increasingly being used for fabrication of engineered tissues for regenerative medicine, drug testing, and other biomedical applications. The success of this technology lies with the development of suitable bioinks and hydrogels that are specific to the intended tissue application. For applications such as neural tissue engineering, conductivity plays an important role in determining the neural differentiation and neural tissue regeneration. Although several conductive hydrogels based on metal nanoparticles (NPs) such as gold and silver, carbon-based materials such as graphene and carbon nanotubes and conducting polymers such as polypyrrole (PPy) and polyaniline were used, they possess several disadvantages. The long-term cytotoxicity of metal nanoparticles (NPs) and carbon-based materials restricts their use in regenerative medicine. The conductive polymers, on the other hand, are non-biodegradable and possess weak mechanical properties limiting their printability into three-dimensional constructs. The aim of this study is to develop a biodegradable, conductive, and printable hydrogel based on collagen and a block copolymer of PPy and polycaprolactone (PCL) (PPy-block-poly(caprolactone) [PPy-b-PCL]) for bioprinting of neural tissue constructs. The printability, including the influence of the printing speed and material flow rate on the printed fiber width; rheological properties; and cytotoxicity of these hydrogels were studied. The results prove that the collagen/PPy-b-PCL hydrogels possessed better printability and biocompatibility. Thus, the collagen/PPy-b-PCL hydrogels reported this study has the potential to be used in the bioprinting of neural tissue constructs for the repair of damaged neural tissues and drug testing or precision medicine applications.

Keywords: Three-dimensional printing; Tissue engineering scaffolds; Peripheral nerve injury; Nerve guide conduit; Conductive scaffolds; Stem cells

*Correspondence to: Sanjairaj Vijayavenkataraman, Department of Mechanical Engineering, National University of Singapore, Singapore; vijayavenkataraman@u.nus.edu and Wen Feng Lu, Department of Mechanical Engineering, National University of Singapore, Singapore; mpelwf@nus.edu.sg

Received: May 23, 2019; **Accepted:** June 26, 2019; **Published Online:** July 11, 2019

(This article belongs to the *Special Issue: Bioprinting in Asia*)

Citation: Vijayavenkataraman S, Vialli N, Fuh JYH, *et al.*, Conductive collagen/polypyrrole-b-polycaprolactone hydrogel for bioprinting of neural tissue constructs. *Int J Bioprint*, 5(2.1): 229. <http://dx.doi.org/10.18063/ijb.v5i2.1.229>.

1. Introduction

Bioprinting is a pioneering technology that aids in the fabrication of biomimetic tissue constructs and expected to provide an effective solution for the long-standing crisis of organ shortage for tissue/organ transplantation^[1]. Development of suitable bioinks is critical for successful adoption of this technology in the field of tissue engineering and regenerative medicine. Hydrogels, which are highly

hydrated polymeric networks, are commonly used as bioinks for bioprinting of tissue constructs due to their structural similarity to a cell's natural extracellular matrix^[2]. Collagen (Type I), gelatin, alginate (Alg), hyaluronic acid, and agarose are the most commonly used naturally-derived hydrogels for bioprinting. Synthetic materials such as poloxamers and poly(ethylene glycol) are also used as hydrogels widely. Although all these hydrogels are hydrophilic, biocompatible, and can be used as bioinks for

encapsulation of cells and bioprinting into tissue constructs, it is important to develop tissue-specific hydrogels for better biomimicry^[3]. For nervous tissue, it is widely reported that a conductive environment promotes neuronal proliferation and differentiation^[4,5]. Hence, the development of conductive hydrogels becomes important and would take the bioprinting of neural tissues to the next level.

Conductivity can be rendered to the hydrogels by incorporation of metal NPs, carbon-based materials, and conductive polymers. Metal NPs such as gold NPs^[6], silver NPs^[7], and metal oxide NPs such as zirconia NPs^[8] and iron oxide NPs^[9] were widely used in the preparation of conductive hydrogels. The advantages of using these NPs are their electrical conductivity, magnetic properties, and antibacterial properties, and these properties can be tuned by varying the shape and size of the NP^[10]. Carbon-based materials such as graphene^[11], graphene oxide^[12], reduced graphene oxide^[13], and carbon nanotubes^[14] are another category of materials that are used in the making of conductive hydrogels. Carbon-based materials possess several advantages such as excellent biocompatibility, variety of physical and chemical properties, high surface area, and conductivity. Despite the advantages of metal NPs and carbon-based materials, their application in the area of tissue engineering and regenerative medicine is limited due to their long-term cytotoxicity^[10].

Conductive polymers are the third category of materials that are used for the preparation of conductive hydrogels. These polymers include polypyrrole (PPy), polyaniline (PANI), polythiophene (PT), and poly(3,4-ethylenedioxythiophene) (PEDOT). Many conductive hydrogels using these conductive polymers have been reported in literature. Yang *et al.*^[15] reported electrically conductive PPy/Alg hydrogels and found that these hydrogels promote the cell adhesion, growth, and neural differentiation of human bone marrow-derived mesenchymal stem cells (hMSCs). Another PANi-based hydrogel gellan gum/PANI was reported^[16] to enhance the C2C12 myoblasts proliferation and myosin expression. Another example is the electroconductive hydrogel based on functional poly(ethylene dioxythiophene)^[17] that promoted the proliferation and differentiation of C2C12 cells. Although the conductive polymers based hydrogels are better than the metal NP-based hydrogels and carbon-based material hydrogels in terms of its long-term cytocompatibility, these conducting polymers are non-biodegradable while biodegradability is a desired property in tissue engineering constructs.

To address the above concern, a biodegradable and conductive block copolymer of PPy and PCL, PPy-b-PCL is used in this study. Three different concentrations of PPy-b-PCL (0.5, 1, and 2%) were mixed with collagen (Type I) to prepare the hydrogels, the rheological characteristics, printability, and cytocompatibility were examined, with pure collagen hydrogel being used as the control.

2. Experimental Section

2.1 Materials

Rat Tail Collagen Type I (Corning #354236, 3-4 mg/ml in 0.02 N acetic acid) and PPy-b-PCL (Sigma-Aldrich Pte Ltd., Singapore) were used for the preparation of the bioink.

2.2 Preparation of Collagen and Collagen/PPy-b-PCL Solution

A concentration of 4% (w/v) Collagen Type 1 was used. Minimum essential medium was added to 4% (w/v) collagen solution and mixed well, which was used as the control. Three different concentrations (0.5, 1, and 2%) of PPy-b-PCL were added to the collagen bioink. The bioink was then neutralized with 1M sodium hydroxide (NaOH). The conductivity of the prepared bioinks was measured using a conductivity meter (SevenCompact™ pH/Ion meter S220, Mettler-Toledo Singapore Pte Ltd., Singapore) and the conductivity of the collagen/PPy-b-PCL bioinks was in the order 1-5 mS/cm while pure collagen bioink had negligible conductivity values.

2.3 (Bio)Printing of Collagen and Collagen/PPy-b-PCL Scaffolds

An in-house built bioprinting system (Figure 1) was used for the printing of bioinks. The main components of the system are the high precision XYZT stage along with the controller, a syringe pump, and a computer. The schematic of the bioprinting set-up and the image of the actual in-house built bioprinting system are shown in Figure 1A and B, respectively. The XYZT stage was driven by linear motors, with the X- and Y-axis having a travel distance of 150 mm with $\pm 5 \mu\text{m}$ accuracy. The travel distance of Z-axis was 50 mm with $\pm 2 \mu\text{m}$ accuracy. Software for stage control, connecting tubes, syringes, and needles are other components. A 13 mm internal diameter syringe and 0.5 mm internal diameter needle were used in all the experimental trials. Glass Petri dishes of diameter 100 mm were used as substrates for printing. After printing, the constructs were left to gel in the fridge at 4°C for 3 h before it was taken out for further testing.

2.4 Rheological Characterization

The rheological properties of collagen and collagen/PPy-b-PCL bioink were assessed using a parallel plate rheometer (DHR-3, TA Instruments, USA). The bioink samples for rheological characterization are 30 mm in diameter and 1 mm in thickness (Figure 2). The temperature of the plate was set to 25°C. The top plate was lowered to a height of 1500 μm . Frequency and strain sweep tests were performed. For frequency sweep,

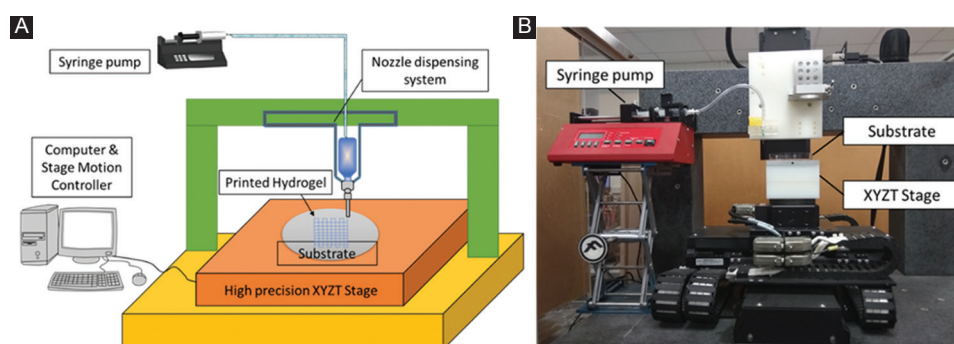


Figure 1. (A) Schematic of the bioprinting set-up and (B) image of the actual in-house built bioprinting system.

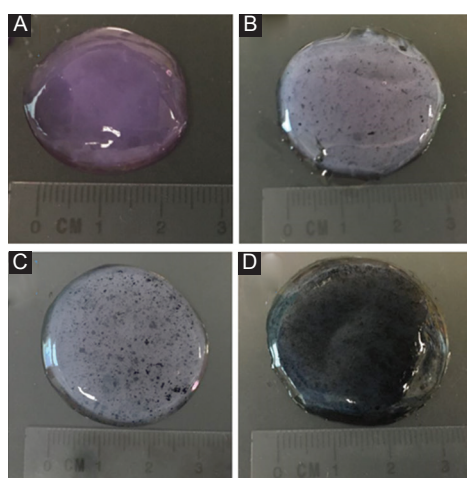


Figure 2. Samples of (A) collagen, (B) collagen/0.5% polypyrrole-block-poly(caprolactone) (PPy-b-PCL), (C) collagen/1% PPy-b-PCL, and (D) collagen/2% PPy-b-PCL bioink for rheological characterization.

the dynamic storage and loss moduli were evaluated at 1% strain amplitude at a frequency ranging from 0.01 to 100 Hz. For the strain sweep test, the moduli were evaluated at strain amplitude ranging from 0 to 1000% at 1Hz. The average fiber diameter and pore size were calculated from the images using an image analysis software (ImageJ, National Institute of Health, Bethesda, MD).

2.5 Fiber Fusion Test

Two consecutive layers of collagen, collagen/0.5% PPy-b-PCL, collagen/1% PPy-b-PCL, and collagen/2% PPy-b-PCL bioink were fabricated layer by layer to conduct the fiber fusion test. The fabricated structure follows zero degree and an orthogonal pattern and increasing fiber to fiber distance (FD). The range of fiber to FD used in this study is 2-10 mm with 2 mm increments. After considering the fiber diameter (d_p), the raster width is defined as, $R_w = FD - d_p$, as shown in Figure 3. The printing speed, material flow rate, nozzle diameter, and print distance used in this test are 7 mm/s, 3 ml/min, 0.8 mm,

and 1 mm, respectively, and images were taken. The percentage of diffusion rate (rate of material spreading) (Df_r) is determined^[18] using Equation (1):

$$Df_r = \frac{A_t - A_A}{A_A} \times 100\% \quad (1)$$

Where A_t and A_A are theoretical and the actual areas of the pores, respectively. When $A_t = A_A$, the diffusion rate of the pore is zero, without any material spreading.

2.6 Bioprinting of Cell Laden Collagen and Collagen/PPy-b-PCL Conductive Bioink and *In Vitro* Studies

The PC12 cells (a cell line derived from a pheochromocytoma of the rat adrenal medulla) were maintained in Dulbecco's modified Eagle's medium high glucose, supplemented with 10% fetal bovine serum, 5% horse serum, and 1% penicillin/streptomycin. The PC12 cells were incubated at 37°C in a humidified atmosphere containing 5% CO₂ and the culture medium was replaced every 2nd day. After reaching 70-80% confluence, the cells were detached by trypsin EDTA, and viable cells were counted by a trypan blue assay. Dissociated cells were pelleted by centrifugation at 2000 rpm for 5 min. The pellet was suspended in the collagen and collagen/PPy-b-PCL bioink at a density of 1×10^5 cells per ml and printed using the in-house built bioprinter. The printed structures were 2 cm×2 cm in size and a pore size of 1 mm. The cell-laden constructs were left in an incubator at 37°C in a humidified 5% CO₂ environment for 2 days to proliferate.

The cytotoxicity was evaluated by determining cell viability after 48 h of incubation. The number of viable cells was determined by estimating their mitochondrial reductase activity using the PrestoBlue (Thermo Fisher Scientific, Waltham, MA, USA) with a microplate reader at a wavelength of 570 nm. Culture media were set as the blank. Absorbance was measured at a wavelength of 570 nm using a microplate spectrophotometer (Tecan,

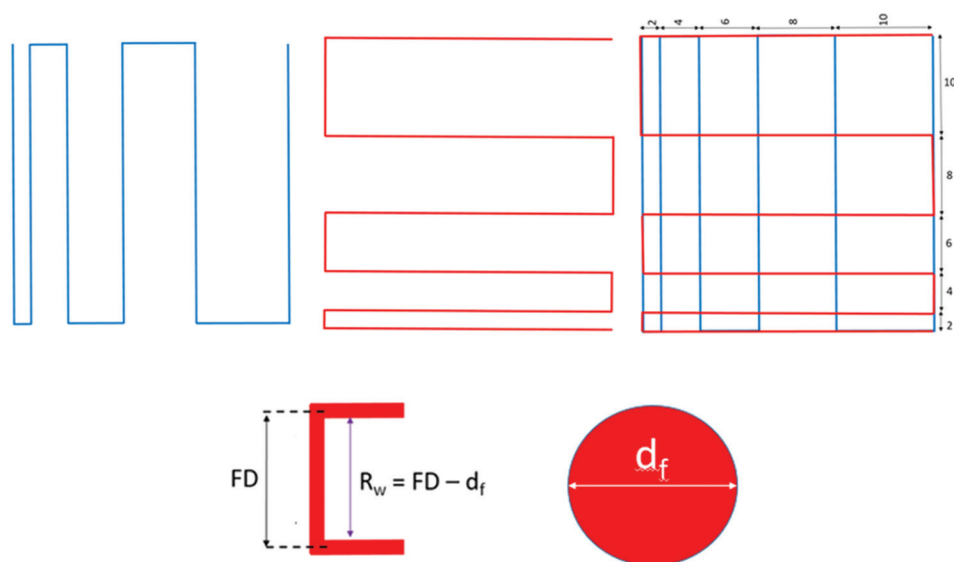


Figure 3. Printing design for fiber fusion test and calculation of fiber width. Two consecutive layers (first layer in blue and second layer in red) of the different bioinks were fabricated layer by layer. The fabricated structure follows zero degree and an orthogonal pattern and increasing fiber to FD. The range of fiber to fiber distance used in this study is 2-10 mm with 2 mm increments.

200 Infinite Pro, Männedorf, Switzerland). Experiments were performed in triplicates.

2.7 Statistical Analysis

Experiments were run in triplicates, and all measurements were expressed as mean \pm SD. One-way ANOVA test was used to determine any significant differences existed between the mean values of the experimental groups. Differences were considered statistically significant at $P < 0.05$.

3. Results

3.1 Influence of Printing Speed and Material Flow rate on Fiber Width

The influence of two main factors that determine the fiber width, namely, the printing speed and material flowrate, was studied. First, for each composition of the bioink, a single layer line having 20 mm length is deposited with various printing speeds (i.e., 1, 3, 5, 7, and 10 mm/s). The material flow rate used for this test is 3 ml/min. Second, for each composition of the hydrogel, a single layer line having 20 mm length is deposited with various flow rates (i.e., 1, 3, 5, 7, and 10 ml/min). The printing speed used for this test was 5 mm/s. For these two tests, the nozzle diameter and print distance used for this test are 0.8 mm and 1 mm, respectively. The width of the fiber is measured with microscopic imaging.

The effect of printing speed on fiber width is shown in Figure 4A and Table S1 (supplementary information). With increasing printing speed, the fiber width decreases for all hydrogel compositions tested. The printing speed

affects the hydrogel deposition and as it increases, the hydrogel deposition experiences some tension and becomes thinner. Higher printing speed may break the continuous line printing deposition of the hydrogel. The addition of PPy-b-PCL with collagen generally results in larger fiber width. This could be due to the higher viscosity of hydrogel composition, resulting in inhomogeneous line printing and lead to the higher value of fiber width. The collagen/PPy-b-PCL composition results in an overall better printing result are shown in Table S1 (supplementary information), where the continuous line is produced at printing speed 3 mm/s and above.

The effect of material flow rate on fiber width is shown in Figure 4B and Table S2 (supplementary information). With increasing material flow rate, the fiber width generally increases for all bioink compositions tested. When the material flow rate is increased, the amount of bioink deposited increases and thereby resulting in a thicker fiber. For all the bioink compositions, the fiber width is much higher than the nozzle diameter due to the relatively low printing speed (5 mm/s). Similar observation mentioned earlier is seen here as well, in which the addition of PPy-b-PCL to collagen results in thicker fibers. It is also observed that at higher material flow rates, during printing or right after the line is printed, the bioink clumps into an irregular shape at some intervals rather than forming a continuous line. The optimal material flow rate observed here for the line printing to produce a continuous line with minimum spreading is 5 ml/min.

Furthermore, varying the printing speed and material flow rate of the bioink plays a role in the curvature of the corners of the deposited fiber. In Table 1, it is evident

that the corner of the deposited fiber width changes from a sharp to round curves as the printing speed decreases. Fiber deposited at higher speed increases the accuracy of the designed fiber width as compared to those deposited at lower speeds, where there is a higher chance of material accumulation at the corners due to the lower speed.

In Table 2, it is shown that the corner of the deposited fiber changes from a sharp to round curves as the material flow rate increases. Fibers deposited with lower material flow rate increases the accuracy of the designed fiber width as compared to those deposited with higher material flow rate, where there is a higher chance of material accumulation at the corners due to the higher material flow rate.

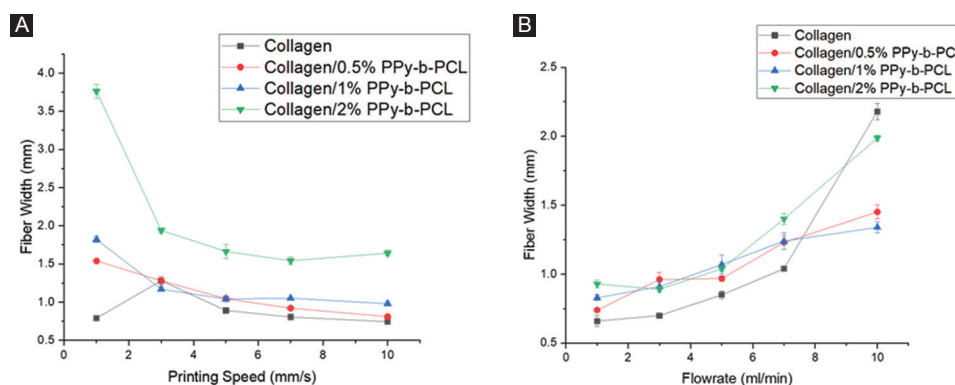


Figure 4. Influence of (A) printing speed on fiber width at a constant material flow rate of 3 ml/min and (B) material flow rate on fiber width at a constant printing speed of 5 mm/s.

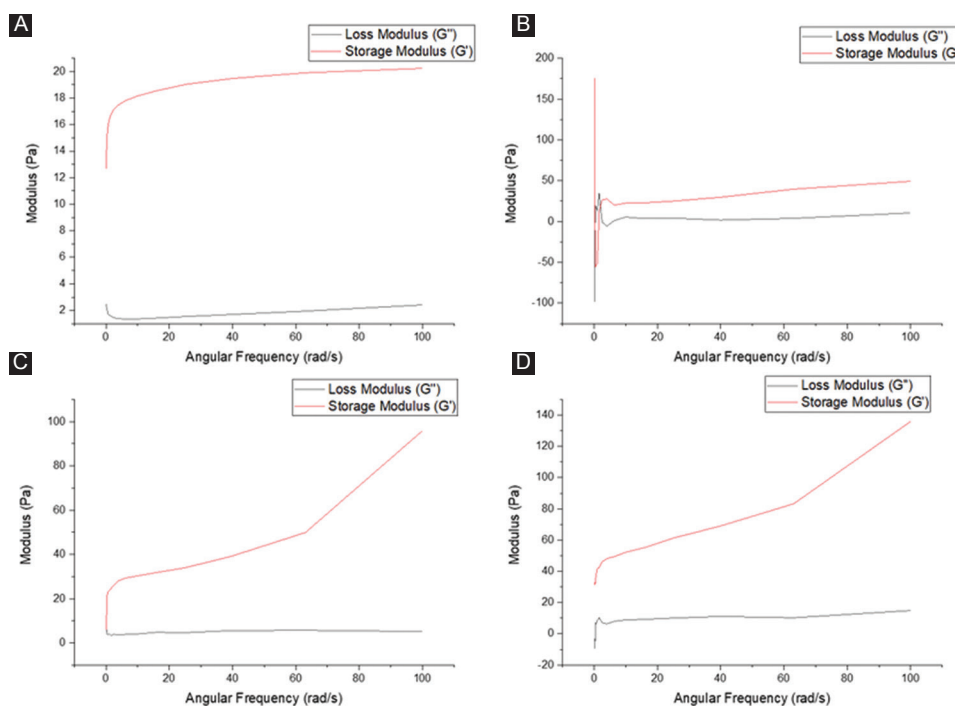
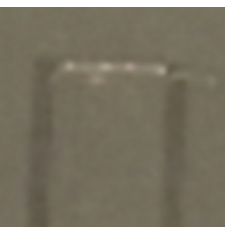


Figure 5. Rheological studies – frequency sweep (A) collagen, (B) collagen/0.5% PPy-block-poly(caprolactone) (PPy-b-PCL), (C) collagen/1% PPy-b-PCL, and (D) collagen/0.5% PPy-b-PCL.

Table 1. Influence of printing speed on fiber corners at a constant material flow rate of 3 ml/min.

Bioink	Printing speed (mm/s)				
	1	3	5	7	10
Collagen					
Collagen/0.5% PPy-b-PCL					
Collagen/1% PPy-b-PCL					
Collagen/2% PPy-b-PCL					

PPy-b-PCL: PPy-block-poly (caprolactone)

value, with collagen/2% PPy-b-PCL bioink the highest, which shows that the mechanical integrity of the collagen hydrogel increases with increasing concentration of PPy-b-PCL. The strain sweep results are shown in Figure 6. In general, the storage modulus G' is higher than the loss modulus G'' then it crosses and the loss modulus G'' is higher at the oscillation percentage range of 150-1000, where the microstructure collapses and the material flows. The modulus crossing point value is generally higher in the bioinks containing PPy-b-PCL, the highest being collagen/2% PPy-b-PCL bioink.

3.3 Fiber Fusion Tests

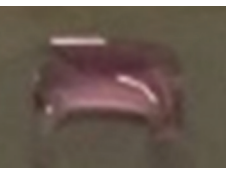
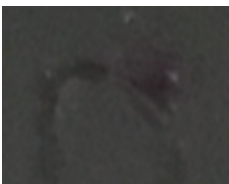
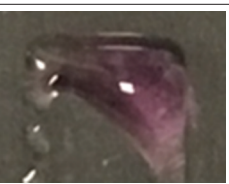
Qualitatively, the collagen/PPy-b-PCL composition generally shows a good printable pore size, as shown in Figure 7A-D. The higher the diffusion rate, the higher the amount of material spread during printing. Thus, the lowest diffusion rate is desired for printing desired pore size ($D_f=0$). For all the composition, pore size 2×2

and $4 \times 4 \text{ mm}^2$ has a very low printability as the material spread widely during printing, closing the pore. As the pore size is increased, the diffusion rate of the material shows a decreasing trend, as shown in Figure 7E. The collagen/0.5% PPy-b-PCL and collagen/1% PPy-b-PCL composition show the least material spreading after printing, producing the best square geometry of the pore. The test results corroborate the rheological properties measured, showing that the collagen/PPy-b-PCL composition has higher mechanical integrity.

3.4 Bioprinting and Cell Culture Studies

PC12 cells were suspended in the collagen and collagen/PPy-b-PCL hydrogels and were bioprinted. The printed constructs were incubated for 48 h and the cell viability was determined using the PrestoBlue assay. The results of the cytotoxicity test are shown in Figure 7F. The results reveal that the addition of PPy-b-PCL to collagen was not toxic to the PC12 cells, and the cell viability between

Table 2. Influence of material flow rate on fiber corners at a constant printing speed of 5 mm/s.

Bioink	Material flow rate (ml/min)				
	1	3	5	7	10
Collagen					
Collagen/0.5% PPy-b-PCL					
Collagen/1% PPy-b-PCL					
Collagen/2% PPy-b-PCL					

PPy-b-PCL: PPy-block-poly (caprolactone)

collagen and collagen/PPy-b-PCL hydrogels does not differ significantly. Further detailed studies on neural differentiation of PC12 cells or other primary neural stem cells (NSC) with gene and protein characterization has to be done in the future to evaluate the effectiveness of these conductive bioinks in the neural differentiation process.

4. Discussion

Conductive collagen/PPy-b-PCL hydrogels were reported in this study. These hydrogels are both conductive and biodegradable unlike the other non-biodegradable but conductive hydrogels based on PPy, PANi, PT, and PEDOT. The influence of printing speed and material flow rate on the printed fiber width, rheological characteristics, fiber fusion, and diffusion rate after printing, and cytotoxicity of these hydrogels were evaluated.

Collagen is one of the most widely used natural polymers in tissue engineering applications due to the many advantages it possesses. First, collagen is the main protein of the cell's extracellular matrix^[20] and hence, using collagen would offer a biomimetic environment for the cells to grow and proliferate. Second, collagen supports better cell attachment and integrin signaling

due to the presence of native binding motifs^[21]. Third, collagen can be cross-linked using various cross-linking mechanisms such as UV crosslinking, thermal gelation^[22], and chemical cross-linking using formaldehyde or glutaraldehyde^[23]. Cross-linking is an important step in bioprinting as it determines the structural integrity of the printed construct. Since collagen could be cross-linked with a variety of cross-linking mechanisms, it offers a significant advantage. Finally, collagen is a soft material with an elastic modulus of <5 kPa^[24]. It is known that neural cells prefer softer substrates (elastic moduli 1-10 kPa)^[19]. When stem cells are used in bioprinting, and the cells are expected to differentiate into the neural lineage, the stiffness of the hydrogels used for encapsulation of stem cells determines to a greater extent the fate of the stem cell differentiation. Since the intended application of this study is neural tissue, choice of collagen-based hydrogel is justified.

There were several studies that reported the enhanced neural cell proliferation and neuron differentiation on conductive substrates. Shi *et al.*^[25] prepared electrically conductive nanoporous cellulose gels (NCG)/PPy composite hydrogels using NCG and PPy NPs and it was

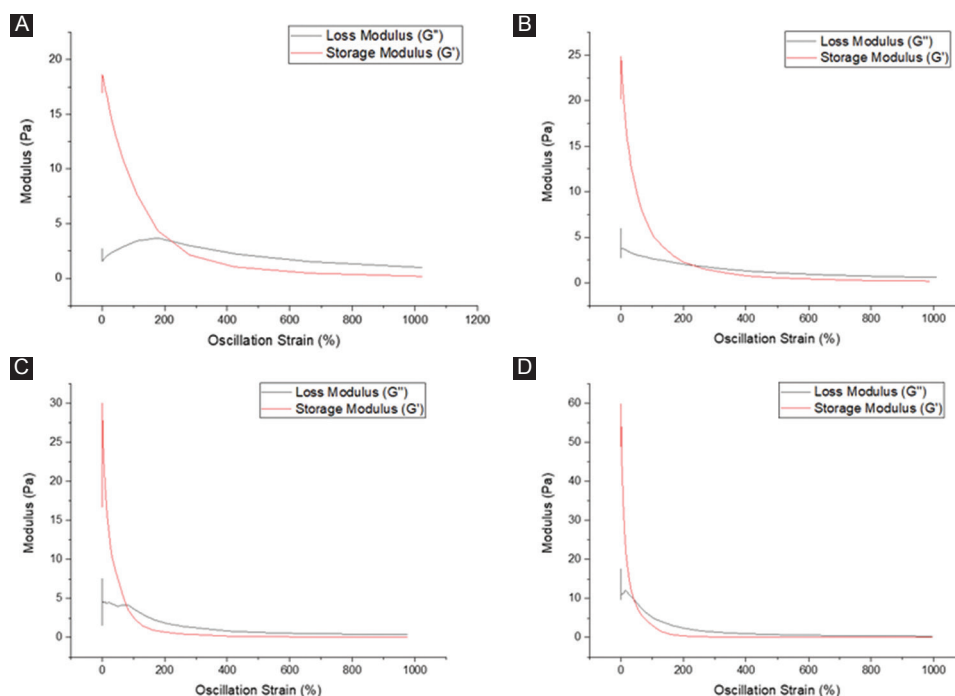


Figure 6. Rheological studies – strain sweep (A) collagen, (B) collagen/0.5% PPy-block-poly(caprolactone) (PPy-b-PCL), (C) collagen/1% PPy-b-PCL, and (D) collagen/2% PPy-b-PCL.

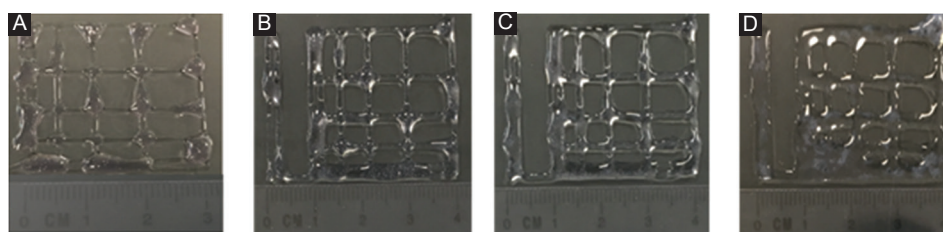
found that this conductive hydrogel resulted in enhanced adhesion and proliferation of PC12 cells compared to the non-conductive NCG hydrogel. Another conductive composite hydrogel made of sodium Alg, carboxymethyl chitosan polymer, and PPy was developed by Bu *et al.*^[26]. The *in vitro* studies using PC12, RSC96, and hMSCs and *in vivo* studies with adult Sprague-Dawley rats confirmed the biocompatibility of this hydrogel and its role in the neural tissue regeneration. In another study^[27], a polyurethane (PU) hybrid composite hydrogel comprising PU, PEDOT: PSS, and liquid crystal graphene oxide were found to support the human NSC growth and also its differentiation to neurons and supporting neuroglia.

While all these studies using several conductive polymers such as PPy, PANi, PT, and PEDOT proved their excellent biocompatibility and had been used previously as substrates for neural cell/tissue culture, they are non-biodegradable and possess weak mechanical properties limiting its printability into three-dimensional structures^[28]. The block copolymer of PPy and PCL used in this study is biodegradable and blending the PPy-b-PCL with collagen improves its printability. The conductivity of the collagen/PPy-b-PCL hydrogels developed in this study was in the order of 1-5 mS/cm. From the printability studies and rheological characterizations, it is found that the collagen/PPy-b-PCL hydrogels could be bioprinted with good structural integrity and better than pure collagen hydrogel. The cytotoxicity studies also

confirm that the cells are not significantly affected with the addition of PPy-b-PCL and further detailed *in vitro* and *in vivo* studies are required to prove the effectiveness of these hydrogels in enhancing the neural differentiation.

5. Conclusion

A biodegradable and conductive hydrogel based on collagen/PPy-b-PCL composites was developed to be used as a bioink for encapsulation of cells in the bioprinting process. The printability of the hydrogels was studied. The fiber width decreases with increasing printing speed as expected. The addition of PPy-b-PCL with collagen generally results in larger fiber width. This could be due to the higher viscosity of hydrogel composition, resulting in inhomogeneous line printing, which, in turn, leads to a higher value of the fiber width. The collagen/PPy-b-PCL composition results in an overall better printing, and continuous line is produced at a printing speed of 3 mm/s and above. With increasing material flow rate, the fiber width generally increases for all bioink compositions tested. The optimal material flow rate observed for the line printing to produce a continuous line with minimum diffusion is 5 ml/min. From the rheological studies, the storage modulus G' is higher than the loss modulus G'' in all the compositions tested, which shows that the material has an elastic-solid behavior and is highly structured. It is also observed that the bioink with the addition of PPy-b-PCL has higher modulus value; thus, the mechanical integrity of the collagen hydrogel increases with increasing



Pore size (mm x mm)	Diffusion rate (%)			
	Collagen	Collagen/0.5% PPy-b-PCL	Collagen/1% PPy-b-PCL	Collagen/2% PPy-b-PCL
2 x 2	100.00	100.00	100.00	100.00
4 x 4	100.00	100.00	100.00	100.00
6 x 6	37.50	38.89	37.50	100.00
8 x 8	34.38	12.50	6.25	60.94
10 x 10	28.00	14.50	9.75	44.00

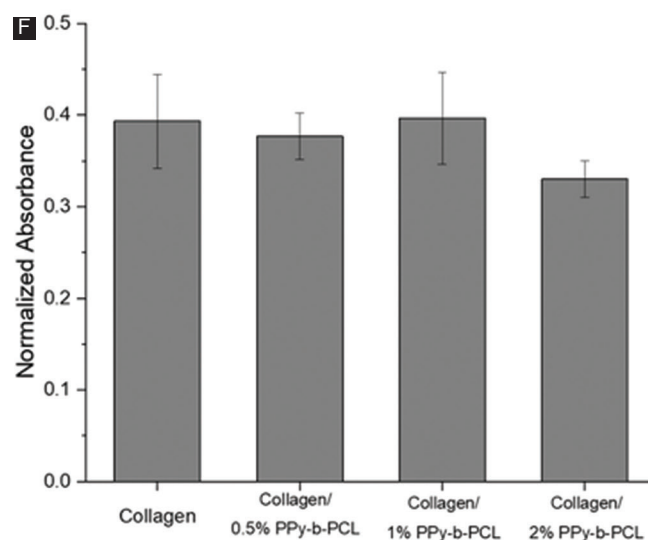


Figure 7. (A–D) Images of fiber fusion tests of (A) collagen, (B) collagen/0.5% PPy-block-poly(caprolactone) (PPy-b-PCL), (C) collagen/1% PPy-b-PCL, (D) collagen/2% PPy-b-PCL, (E) diffusion rate in printed hydrogel constructs of various pore sizes, and (F) cytotoxicity results of bioprinted constructs with PC12 cells using PrestoBlue assay after 48 h.

concentration of PPy-b-PCL. The collagen/0.5%PPy-b-PCL and collagen/1%PPy-b-PCL composition shows the least material spreading after printing, producing the best square geometry of the pore. The cytotoxicity studies confirm that the cells are not significantly affected by the addition of PPy-b-PCL.

Funding

This research was funded by the Agency for Science, Technology, and Research (A*STAR) Advanced Manufacturing and Engineering Research Grant R-265-000-630-305.

References

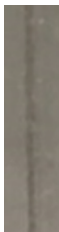
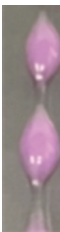
1. Vijayavenkataraman S, Yan WC, Lu WF, *et al.*, 2018, 3D Bioprinting of Tissues and Organs for Regenerative Medicine. *Advanced Drug Delivery Reviews*, 132:296-332. DOI 10.1016/j.addr.2018.07.004.
2. Merceron TK, Murphy SV, 2015, *Hydrogels for 3D Bioprinting Applications, Essentials of 3D Biofabrication and Translation*. San Diego: Elsevier, pp. 249-70. DOI 10.1016/b978-0-12-800972-7.00014-1.
3. Skardal A, Devarasetty M, Kang HW, *et al.*, 2016, Bioprinting

- Cellularized Constructs using a Tissue-specific Hydrogel Bioink. *Journal of Visualized Experiments*, 110:e53606. DOI 10.3791/53606.
4. Vijayavenkataraman S, Thaharah S, Zhang S, *et al.*, 2019, Electrohydrodynamic Jet 3D-printed PCL/PAA Conductive Scaffolds with Tunable Biodegradability as Nerve Guide Conduits (NGCs) for Peripheral Nerve Injury Repair. *Materials and Design*, 162:71-184. DOI 10.1016/j.matdes.2018.11.044.
 5. Vijayavenkataraman S, Thaharah S, Zhang S, *et al.*, 2018, 3D-Printed PCL/rGO Conductive Scaffolds for Peripheral Nerve Injury Repair. *Artificial Organs*, 43(5):515-23. DOI 10.1111/aor.13360.
 6. Xing R, Liu K, Jiao T, *et al.*, 2016, An Injectable Self-Assembling Collagen Gold Hybrid Hydrogel for Combinatorial Antitumor Photothermal/Photodynamic Therapy. *Advanced Materials*, 28(19):3669-76. DOI 10.1002/adma.201600284.
 7. Xu L, Li X, Takemura T, *et al.*, 2012, Genotoxicity and Molecular Response of Silver Nanoparticle (NP)-based Hydrogel. *Journal of Nanobiotechnology*, 10(1):16. DOI 10.1186/1477-3155-10-16.
 8. Zare M, Ramezani Z, Rahbar N, 2016, Development of Zirconia Nanoparticles-decorated Calcium Alginate Hydrogel Fibers for Extraction of Organophosphorous Pesticides from Water and Juice Samples: Facile Synthesis and Application with Elimination of Matrix Effects. *Journal of Chromatography A*, 1473:28-37. DOI 10.1016/j.chroma.2016.10.071.
 9. Paquet C, de Haan HW, Leek DM, *et al.*, 2011, Simard, Clusters of Superparamagnetic Iron Oxide Nanoparticles Encapsulated in a Hydrogel: A Particle Architecture Generating a Synergistic Enhancement of the T2 Relaxation. *ACS Nano*, 5(4):3104-12. DOI 10.1021/nn2002272.
 10. Min J, Patel M, Koh WG, 2018, Incorporation of Conductive Materials into Hydrogels for Tissue Engineering Applications. *Polymers*, 10(10):1078. DOI 10.3390/polym10101078.
 11. Lee WC, Lim CHY, Shi H, *et al.*, 2011, Origin of Enhanced Stem Cell Growth and Differentiation on Graphene and Graphene Oxide. *ACS Nano*, 5(9):7334-41. DOI 10.1021/nn202190c.
 12. Jing X, Mi HY, Napiwocki BN, *et al.*, 2017, Turng, Mussel-inspired Electroactive Chitosan/Graphene Oxide Composite Hydrogel with Rapid Self-healing and Recovery Behavior for Tissue Engineering. *Carbon*, 125:557-570. DOI 10.1016/j.carbon.2017.09.071.
 13. Shin SR, Zihlmann C, Akbari M, *et al.*, 2016, Reduced Graphene Oxide-gelMA Hybrid Hydrogels as Scaffolds for Cardiac Tissue Engineering. *Small*, 12(27):3677-89. DOI 10.1002/smll.201600178.
 14. Sun H, Zhou J, Huang Z, *et al.*, 2017, Carbon Nanotube-incorporated Collagen Hydrogels Improve Cell Alignment and the Performance of Cardiac Constructs. *International Journal of Nanomedicine*, 12:3109. DOI 10.2147/ijn.s128030.
 15. Yang S, Jang L, Kim S, *et al.*, 2016, Polypyrrole/Alginate Hybrid Hydrogels: Electrically Conductive and Soft Biomaterials for Human Mesenchymal Stem Cell Culture and Potential Neural Tissue Engineering Applications. *Macromolecular Bioscience*, 16(11):1653-61. DOI 10.1002/mabi.201600148.
 16. Srisuk P, Berti FV, da Silva LP, *et al.*, 2018, Electroactive Gellan Gum/Polyaniline Spongy-like Hydrogels. *ACS Biomaterials Science and Engineering*, 4(5):1779-87. DOI 10.1021/acsbomaterials.7b00917.
 17. Mawad D, Artzy-Schnirman A, Tonkin J, *et al.*, 2016, Electroconductive Hydrogel Based on Functional Poly (Ethylenedioxy Thiophene). *Chemistry of Materials*, 28(17):6080-8. DOI 10.1021/acs.chemmater.6b01298.
 18. Ribeiro A, Blokzijl MM, Levato R, *et al.*, 2017, Assessing Bioink Shape Fidelity to Aid Material Development in 3D Bioprinting. *Biofabrication*, 10(1):14102. DOI 10.1088/1758-5090/aa90e2.
 19. Engler AJ, Sen S, Sweeney HL, *et al.*, 2006, Matrix Elasticity Directs Stem Cell Lineage Specification. *Cell*, 126(4):677-89. DOI 10.1016/j.cell.2006.06.044.
 20. Lee C.H, Singla A, Lee Y, 2001, Biomedical Applications of Collagen. *International Journal of Pharmaceutics*, 221(1-2):1-22.
 21. Levental KR, Yu H, Kass L, *et al.*, 2009, Matrix Crosslinking Forces Tumor Progression by Enhancing Integrin Signaling. *Cell*, 139(5):891-906. DOI 10.1016/j.cell.2009.10.027.
 22. Lee C, Grodzinsky A, Spector M, 2001, The Effects of Cross-linking of Collagen-glycosaminoglycan Scaffolds on Compressive Stiffness, Chondrocyte-mediated Contraction, Proliferation and Biosynthesis. *Biomaterials*, 22(23):3145-54. DOI 10.1016/s0142-9612(01)00067-9.
 23. Roberts J, Martens P, 2016, Engineering Biosynthetic Cell Encapsulation Systems. In: *Biosynthetic Polymers for Medical Applications*. San Diego: Elsevier, pp. 205-39. DOI 10.1016/b978-1-78242-105-4.00009-2.
 24. Lau YKI, Gobin AM, West JL, 2006, Overexpression of Lysyl Oxidase to Increase Matrix Crosslinking and Improve Tissue Strength in Dermal Wound Healing. *Annals of Biomedical*

- Engineering*, 34(8):1239-46. DOI 10.1007/s10439-006-9130-8.
25. Shi Z, Gao H, Feng J, *et al.*, 2014, *In situ* Synthesis of Robust Conductive Cellulose/Polypyrrole Composite Aerogels and their Potential Application in Nerve Regeneration. *Angewandte Chemie International Edition*, 53(21):5380-4. DOI 10.1002/anie.201402751.
26. Bu Y, Xu HX, Li X, *et al.*, 2018, A Conductive Sodium Alginate and Carboxymethyl Chitosan Hydrogel Doped with Polypyrrole for Peripheral Nerve Regeneration. *RSC Advances*, 8(20):10806-17. DOI 10.1039/c8ra01059e.
27. Javadi M, Gu Q, Naficy S, *et al.*, 2018, Conductive Tough Hydrogel for Bioapplications. *Macromolecular Bioscience*, 18(2): 1700270. DOI 10.1002/mabi.201700270.
28. Guo B, Ma PX, 2018, Conducting Polymers for Tissue Engineering. *Biomacromolecules*, 19(6):1764-82.

Supplementary Information

Table S1. Influence of printing speed on fiber width at a constant material flow rate of 3 ml/min.

Bioink	Printing speed (mm/s)				
	1	3	5	7	10
Collagen					
Collagen/0.5% PPy-b-PCL					
Collagen/1% PPy-b-PCL					
Collagen/2% PPy-b-PCL					

PPy-b-PCL: PPy-block-poly (caprolactone)

Table S2. Influence of material flow rate on fiber width at a constant printing speed of 5 mm/s.

Bioink	Material flow rate (ml/min)				
	1	3	5	7	10
Collagen					
Collagen/0.5% PPy-b-PCL					
Collagen/1% PPy-b-PCL					
Collagen/2% PPy-b-PCL					

PPy-b-PCL: PPy-block-poly (caprolactone)